Face Recognition Based on Local Gradient Number Pattern and Fuzzy Convex-Concave Partition

JUNDING SUN, YANAN LV, CHAOSHENG TANG, HAIFENG SIMA, AND XIAOSHENG WU

School of Computer Science and Technology, Henan Polytechnic University, Jiaozuo 454003, China

Corresponding authors: Junding Sun (sunjd@hpu.edu.cn) and Xiaosheng Wu (wuxs@hpu.edu.cn)

ABSTRACT Face recognition has been deeply studied and widely used in recent years. A novel method, called local gradient number pattern (LGNP), is firstly presented in the paper for face description. For LGNP, the Sobel operator is adopted to extract the local gradient information, and the position of the gray transitions in the local neighborhood is used to form the LGNP code based on the LDP-based methods. Then, the concept of fuzzy convex-concave partition (FCCP) is introduced to fuse the global and regional information based on convex-concave partition (CCP). By the combination of LGNP and FCCP, the proposed descriptor is denoted as FCCP_LGNP. To evaluate the performance of FCCP_LGNP comprehensively, a series of experiments were carried out on four different face databases ORL, CALTECH, GEORGIA, and FACE94, and the results show that FCCP_LGNP is superior to the recent state-of-the-art methods based on hand-crafted features. Even compared with the deep learning methods, VGG16 and ResNet101, the proposed descriptor still shows good performance.

INDEX TERMS Face recognition, local gradient number pattern, fuzzy convex-concave partition, LDP-based methods.

I. INTRODUCTION

Biological features, including human faces, have attracted the attention of many scholars due to their high reliability [1]. Compared with other biometric features, human face contains a lot of detailed information, which is uniqueness for human beings [2], such as eyes, eyebrows and mouths. In addition, because of the low cost of collection and high performance, the face recognition has been commonly applied to surveillance, biometrics, security and other fields [3] in recent years.

The schemes for face recognition can generally be divided into two categories: geometric-based and appearance-based methods [4]. The former uses geometric information to describe the facial features, which incorporates the shape and position of the face into a feature vector [5]. The latter analyzes the face information by means of descriptors, and extracts the whole or local features to represent the changes of the facial appearance [6]. Although face analysis and recognition has made great progress in the past decades, those

challenges are still the big problem in face recognition fields, such as different expressions, backgrounds, and illumination. For face recognition, the most important is to find an effective and robust descriptor, which can effectively extract the resolvable face features and remove the influence of light, noise and expression [7]. Many approaches for face analysis and recognition have been mentioned in the literature, such as, collaborative preserving fisher discriminant analysis (CPFDA) [8], discriminative multi-scale sparse coding (DMSC) [9], two-dimensional quaternion principal component analysis (2D-QPCA) [10], and real-time face recognition using deep learning and visual tracking (RFR-DLVT) [11]. These methods use the global facial information for recognition and they are sensitive to the changes of illumination, partial occlusions, expression and poses. Therefore, local descriptors have been deeply studied in the past decades.

As a typical representative, local binary pattern (LBP) was presented [12], which is simple in principle and low in computational complexity. In addition, it combines structural as well as the statistical features. Because of the advantages of LBP, numerous improved operators have been introduced

---

The associate editor coordinating the review of this manuscript and approving it for publication was Hongjun Su.

in recent years [13]–[16], [48], [49]. In order to achieve multi-resolution analysis, Ojala *et al.* [17] extended LBP from 8-neighborhood to arbitrary circular neighborhoods (R, P), where P and R represent the number of sampling points and the radius respectively. For noise-resistance, Tan and Triggs [18] proposed local ternary pattern (LTP), which extends the binary discriminant to the ternary discriminant, and the modified gradient pattern (MGP) [19] defines a new threshold for binarization on the basis of the modified census transform (MCT).

It is generally known that the edge and direction information is important for image analysis. These features were also incorporated into the extended methods of LBP, such as local maximum edge binary patterns (LMEBP) [20], local edge binary pattern (LEBP) [21], and local tetra patterns (LTrP) [22]. Further, Jabid *et al.* [23] proposed the local directional pattern (LDP) to reduce the influence of the random noise and monotonic illumination changes, which is coded by comparing the edge response values of different directions. However, LDP still produces unreliable codes for the uniform and smooth neighborhoods. Based on LDP, enhanced local directional pattern (ELDP) [24], local direction number (LDN) [25], local direction texture pattern (LDTP) [26], [27], and local edge direction pattern (LEDP) [28] were put forward to overcome the shortcomings. Besides the methods based on local features, the deep learning approaches concerning Convolutional Neural Network (CNN) [29], [30] have emerged in recent years. Those methods can learn high-quality information in face images by training models on a large amount of data. Although CNN-based methods have attracted considerable attention, the research on local features is still continuing [46].

For most of the LDP-based methods, they are actually coded in intensity space, i.e., the size of the edge response value. In contrast, the local gradient number pattern (LGNP), presented in the paper, is coded in gradient space. In other words, the distribution of gray values is considered in the new coding scheme. Comparing with the intensity space, the gradient space can preserve the intrinsic relationship between the pixels in the neighborhood. These intrinsic relationships essentially reveal the underlying structural information of the local neighborhood, which tends to be more discriminative. For the traditional LDP-based variants, they calculate the edge response values by Kirsch template. In difference, LGNP considers the horizontal and vertical directions of the local neighborhoods by Sobel operators [31] to reduce the computational complexity. Further, the fuzzy convex-concave partition (FCCP) is introduced in the paper based on the convex-concave partition [35] to fuse the spatial features of the face images. By the combination of LGNP and FCCP, the novel code, called FCCP_LGNP, is extracted for face recognition.

The rest of this article is based on the following ideas. Section II gives a brief introduction of LDP and its related variants. Section III shows the detailed analysis of the proposed method. The experimental results and conclusions are illustrated in Sections IV and V.

II. BRIEF REVIEW OF LDP AND ITS VARIANTS

LDP assigns an 8-bit binary code to each pixel, which can be obtained by convoluting the local 3×3 neighborhood with the Kirsch templates (Shown in Figure 1).
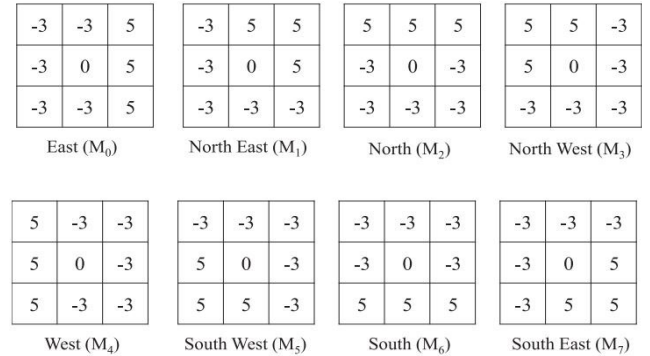

FIGURE 1. Kirsch templates.

Suppose m_i denote the edge response values in i-th direction of a pixel. The top k values $|m_i|$ $(i = 0, 1, \ldots, 7)$ are set to 1, and the remaining $(8-k)$ bits are coded as 0. Then, LDP is defined as,

$$LDP(x, y) = \sum_{i=0}^{7} s(|m_i| - |m_k|) \times 2^i$$

$$s(x) = \begin{cases} 1, & x \geqslant 0 \\ 0, & x < 0 \end{cases} \qquad (1)$$

where $m_i = M_i * I(x_c, y_c)$, $*$ denotes the convolution operation, $I(x, y)$ is a local 3×3 neighborhood centered on (x, y).

Clearly, LDP only considers the size of the edge response values, but not the signs. It is also heavily dependent on the number of prominent edge directions (k). Meanwhile, LDP allocates an 8-bit binary code for each pixel, which easily leads to coding redundancy.

In order to overcome the shortcomings, ELDP was proposed by Zhong and Zhang [24]. For ELDP, the directions corresponding to the largest and the second largest response values are selected to form a double-digit octal number. Different from the coding scheme of ELDP, LDN was proposed by Rivera *et al.* [25], which uses the directions of the maximum and minimum response values for coding. To improve the discrimination ability, LDTP [26] integrates the local direction and the local gray-level information in its coding scheme. Recently, the local directional-structural pattern (LDSP) [32] and the local directional value (LDV) [33] have been proposed. The former uses the position and direction relationship of the edge response values to extract more detailed structural information, and the latter reduces the influence of grayscale variation and noise by combining multi-scale analysis.

III. PROPOSED METHOD

A. LOCAL GRADIENT NUMBER PATTERN

As a vector, the gradient reflects the trend and direction of the spatial gray change, and it can also be used to describe the spatial variations in a local neighborhood. The smaller gradient shows that the point has a uniform local distribution, while the bigger gradient value shows that the point is in a region where the gray level changes rapidly.

In this paper, we propose the local gradient number pattern (LGNP), which computes the gradients in a local neighborhood to describe the gray-value distributions. Essentially, it sharpens the local neighborhood and highlights the transitional part of the gray scale. It reveals the structural relationship among the pixels. By gradients, the edge of the face images can be enhanced, the pattern shadows can be removed and the small mutation in the flat area can be improved.

Let $f(x, y)$ denote the image function, the partial derivative g_x and g_y at each pixel in the neighborhood are given as follows,

$$g_x = \partial f(x, y)/\partial x = f(x + 1, y) - f(x, y)$$
$$g_y = \partial f(x, y)/\partial y = f(x, y + 1) - f(x, y) \quad (2)$$

Then, the gradient can be computed as,

$$G(x, y) = \sqrt{g_x^2 + g_y^2} \quad (3)$$

In order to simplify the calculation and reduce the complexity, we use the following formula to replace the square root operation [50].

$$G(x, y) = |g_x| + |g_y| \quad (4)$$

Obviously, the above procedure can be replaced by means of Sobel operator. Suppose N represents a local 3×3 neighborhood centered on (x, y), G_x and G_y are the gradients in the horizontal and vertical directions respectively. They can be computed as,

$$G_x = \begin{bmatrix} -1 & 0 & 1 \\ -2 & 0 & 2 \\ -1 & 0 & 1 \end{bmatrix} * N, \quad G_y = \begin{bmatrix} 1 & 2 & 1 \\ 0 & 0 & 0 \\ -1 & -2 & -1 \end{bmatrix} * N \quad (5)$$

The gradient G of N are obtained by

$$G = |G_x| + |G_y| \quad (6)$$

As the scheme of ELDP and LDN, the gradient values of the eight directions, are sorted in the order of smallest to largest in size, i.e., $\{g_i\}(i = 1, 2, 3, \ldots, 8)$, and numbered from 0 to 7. Then, the LGNP is coded as
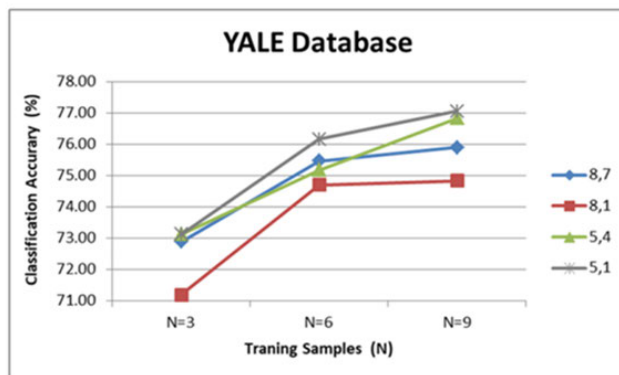
$$LGNP(x, y) = 8 \times d_{g_a} + d_{g_b} \quad (7)$$

where d_{g_a} and d_{g_b} are the directions corresponding to the g_a and g_b, a and b are the sorted indexes ($a, b \in [1, 8]$).

For the traditional LBP and LDP-based operators, they are coded under the topology structure of 3×3 neighborhoods. Ojala et al. [17] presented multi-resolution analysis (R, P) by
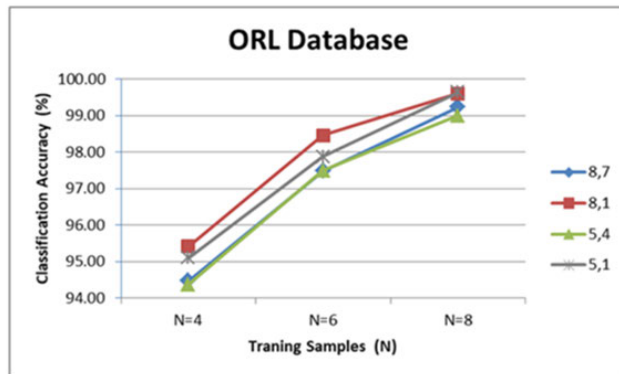

FIGURE 2. Performance comparison for the choice of (a, b). (a) For ORL database. (b) For YALE database.

changing radius R and sample points P in the neighborhood. The feature histograms are extracted under each scale respectively, and then, they are concatenated as the final feature. Obviously, they may produce intractable high dimensionality histograms as the sampling radius increases. To solve the problems, Wu and Sun [34] proposed the joint-scale LBP (JLBP), which fuses different scales by a simple arithmetic operation for feature extraction. In addition, all the multi-scale neighborhoods are reduced to K-neighborhoods before the fusion. Let $[n_{0,R_l}, n_{1,R_l}, \ldots, n_{Kt-1,R_l}]$ denote the $K \times t$ (t is a positive integer) sampled points under the scale $R_l (l = 1, 2, 3, \ldots, L)$, and p_{i,R_l} ($i = 0, 1, 2, \cdots, K$) is the transformed point. Then, p_{i,R_l} can be calculated as

$$p_{i,R_l} = \frac{1}{t} \sum_{x=0}^{t-1} n_{x+t \times i, R_l}, \quad i = 0, 1, \ldots, K - 1 \quad (8)$$

In the paper, K is set to 8, which can realize the convolution easily with the Sobel operator. Obviously, the transformation not only reduces the feature dimensionality, but also improves the robustness to noise by averaging during the transformation process.

As mentioned above, LGNP selects two directions for coding by the gradient values. The gradient values reflect the gray transitions, especially the prominent detail features, such as eye border, lip border, wrinkle, bridge of the nose and etc.
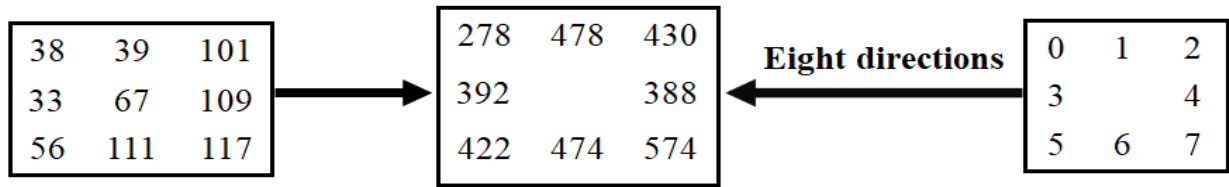
Sorted Index (i)	①	2	3	4	⑤	6	7	8
Gradient values (g_i)	278	388	392	422	430	474	478	574
Directions	0	4	3	5	2	6	1	7

$$LGNP = (20)_8 = 16$$

FIGURE 3. An example of computing LGNP for $(a,b) = (5,1)$.

Obviously, the detailed features play an important role in face recognition. Therefore, the directions, which reflect the gray transitions, are chosen in our coding scheme. Of course, there are many ways to select the two gradient values. Four typical cases are chosen for testing in the paper.

As two typical representatives of the LDP-based methods, the coding schemes of ELDP and LDN are chosen firstly, those are, $(a, b) = (8, 7)$ and $(a, b) = (8, 1)$. Among the gradient values $\{g_i\}(i = 1, 2, 3, \ldots, 8)$, the middle values, g_5 and g_4, divide $\{g_i\}$ into two parts, one is the bigger gradient values including $\{g_6, g_7, g_8\}$, the other is the smaller gradient values including $\{g_1, g_2, g_3\}$. Therefore, $(a, b) = (5, 4)$ is chosen in the testing. In general, smaller gradient values may mean more prominent edge details. Based on this, we consider the combination of the smallest value g_1 and the middle value g_5 for testing, that is, $(a, b) = (5, 1)$.

The performance of the four cases are compared under the scale $(R_l, 8t) = (2, 16)$. The ORL [40] and YALE [43] face databases are chosen as test beds. The experimental results are shown in Figure 2 (a) and (b). It is clear that $(a, b) = (8, 1)$ and $(a, b) = (5, 1)$ get higher scores than the other two conditions for ORL database, and $(a, b) = (5, 1)$ performs best among the four conditions for the more challenging YALE database. Therefore, $(a, b) = (5, 1)$ is selected to form the final LGNP code. Figure 3 gives an example of computing LGNP for $(a,b) = (5,1)$.

B. DEFINITION OF FCCP

For the LBP-based and LDP-based approaches, the neighborhoods with entirely different visual perception may produce the same code [35]. The same is true for LGNP. Figure 4 gives an example, the two neighborhoods (a) and (b) have the same LGNP code (59). To overcome the problem, Sun *et al.* [35] proposed a simple convex-concave partition (CCP) strategy.
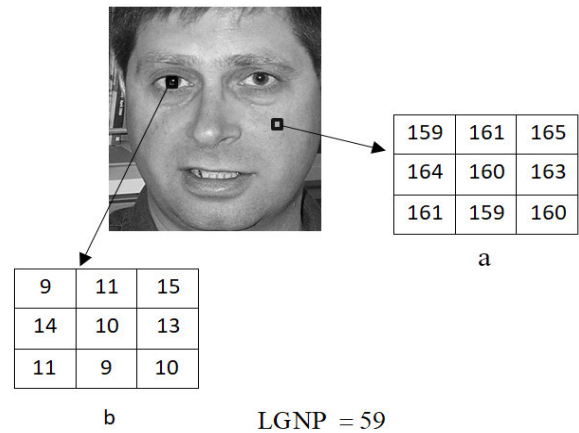
FIGURE 4. Example of the neighborhoods with the same LGNP code.

By CCP, the relative relationship between the local and global gray levels can be obtained, which is helpful to distinguish the patterns with different spatial characteristics.

The CCP uses the gray mean of an image as a threshold to divide a neighborhood into concave or convex type. However, it belongs to hard threshold division. That is to say, if a neighborhood does not belong to concave type, it must belong to convex type, and vice versa. Obviously, a minor change of the gray mean may cause some neighborhoods from concave type to convex type. While, fuzzy set theory [36] provides a way to deal with this kind of problem. The fuzzy local binary patterns (FLBP) is a typical example [37], which uses fuzzy membership function to reduce the sensitivity of LBP to noise and illumination.

Based on the inspiration of FLBP, we also apply the fuzzy membership function to improve the performance of CCP. The new strategy is called fuzzy CCP (FCCP). Let $\mu_{x,y}$ be the
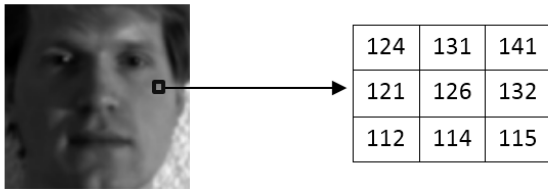
$$CCP : Convex \qquad FCCP \begin{cases} Convex & 0.9745 \\ Concave & 0.0255 \end{cases}$$

FIGURE 5. The comparison of CCP and FCCP.

gray mean of a local neighborhood $N_{(x,y)}$ centered on (x, y), μ and d represent the gray mean and standard deviation of an image respectively, FCCP is defined as,

$$Cov(x, y) = \begin{cases} 0 & if \ \mu_{x,y} - \mu \leqslant -d \\ \frac{1}{2} + \frac{1}{2} \times \frac{\mu_{x,y} - \mu}{d} & if \ -d \leqslant \mu_{x,y} - \mu \leqslant d \\ 1 & if \ \mu_{x,y} - \mu \geqslant d \end{cases}$$

$$Coc(x, y) = 1 - Cov(x, y) \qquad (9)$$

The probability that $N_{(x,y)}$ belongs to convex or concave neighborhood is expressed as $Cov(x, y)$ or $Coc(x, y)$, which is given in Eq. (9).

Figure 5 gives the comparison of CCP and FCCP. The example neighborhood belongs to convex type by CCP. While, FCCP gives two probabilities, which indicate how likely the neighborhood belongs to concave and convex type. Obviously, FCCP is more robust to gray changes and noise.

C. FCCP_LGNP

Based on LGNP and FCCP, the novel operator is given as FCCP_LGNP. Figure 6 depicts the flowchart of computing FCCP_LGNP. The LGNP image is firstly extracted based on the gradient image. Then, the probability of a neighborhood belonging to concave or convex type is calculated based on FCCP. After that, the histograms of concave and convex neighborhoods are computed and fused as the final feature.

D. DISSIMILARTY MEASURE

In general, chi-square statistic is more suitable for measuring the dissimilarity between feature histograms [38]. Therefore, we also choose the measurement. Let $H = \{h_i\}$ and $B = \{b_i\}$ $(i = 1, 2, \ldots, k)$ represent two feature histograms respectively, the chi-square statistic between H and B are computed according to Eq. (10).

$$d_{\chi^2} = \sum_{i=1}^{k} \frac{(h_i - b_i)^2}{h_i + b_i} \qquad (10)$$

IV. EXPERIMENTAL RESULTS
A. EXPERIMENTAL SET-UP

In order to evaluate the performance of the proposed operator FCCP_LGNP, the LDP-based methods are chosen for comparison firstly, including LDP [23], ELDP [24], LDN [25], LDTP [26], MGP [19], LDSP [32], LDV [33] and the central pixel selection (CPS) strategy [39]. For CPS strategy, it was fused with ELDP (called CPS_ELDP in the paper).

We test the approaches on four face databases, ORL [40], CALTECH [41], GEORGIA [42], and FACE94 [44] in the experiment, and $(R_l, 8t)$ was set (1,8), (2,16), (3,24), (4,32),
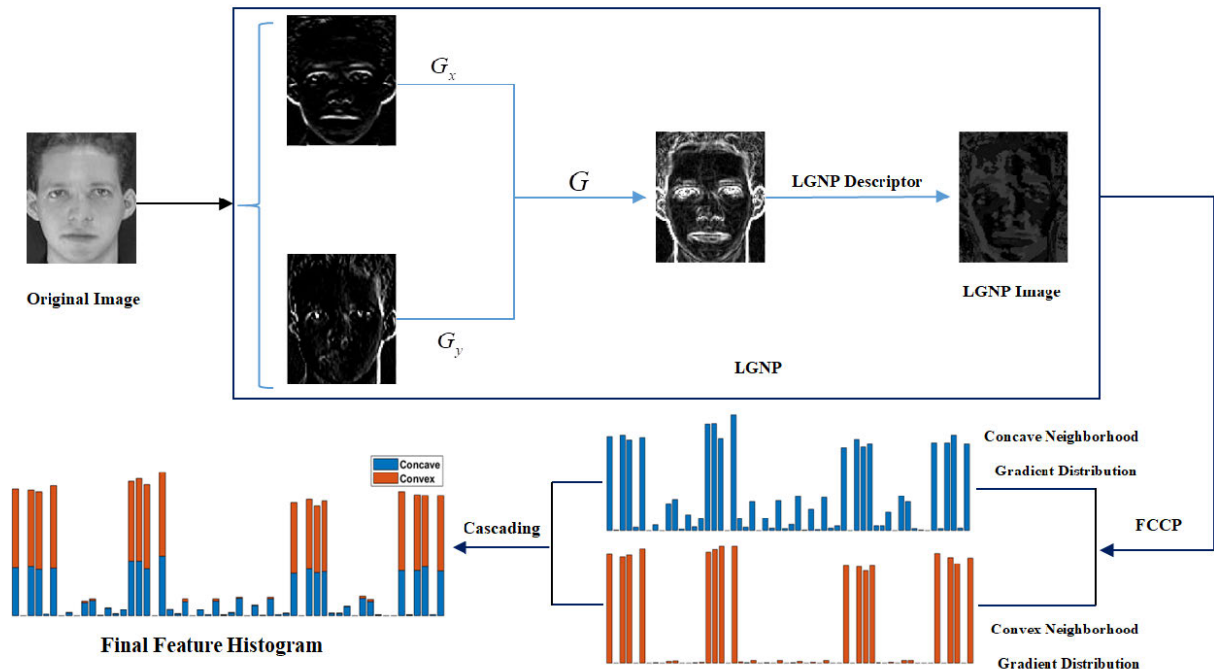

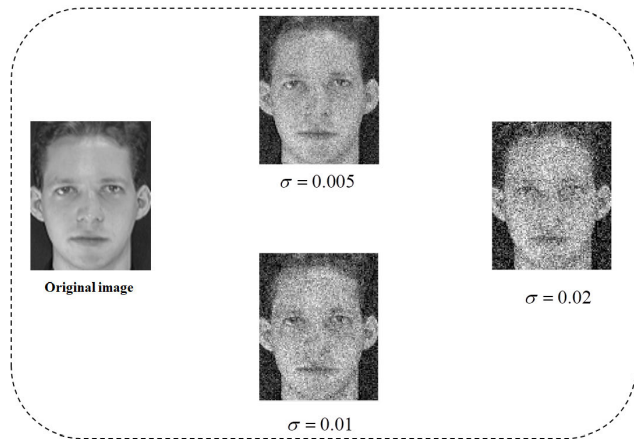**FIGURE 6.** The flowchart of computing FCCP_LGNP.

FIGURE 7. Face images with different noise levels.

FIGURE 8. A volunteer samples from ORL database.

TABLE 1. Experimental results on ORL database.

	N=4							
$(R_l, 8t)$	(1,8)	(2,16)	(3,24)	(4,32)	(5,32)	(6,32)	(7,32)	Avg
LDP	58.98	70.46	79.18	82.24	84.88	86.27	87.62	78.52
ELDP	73.33	81.69	82.61	83.18	83.74	84.52	84.40	81.92
LDN	75.65	84.80	85.49	85.30	86.18	87.00	86.26	84.38
LDTP	83.06	85.71	87.77	88.43	89.91	89.86	89.09	87.69
LDSP	78.68	81.37	80.53	78.54	79.84	79.46	77.75	79.45
MGP	86.83	91.08	91.09	91.66	91.99	91.95	92.27	90.98
LDV	77.65	85.61	86.45	86.00	87.30	87.40	87.10	85.36
CPS_ELDP	91.21	90.87	91.85	91.48	90.93	90.54	89.67	90.93
FCCP_LGNP	**93.34**	**95.11**	**96.04**	**96.64**	**96.83**	**96.28**	**95.60**	**95.69**

	N=6							
$(R_l, 8t)$	(1,8)	(2,16)	(3,24)	(4,32)	(5,32)	(6,32)	(7,32)	Avg
LDP	64.74	77.09	86.27	88.37	90.24	91.73	92.78	84.46
ELDP	80.24	88.64	89.47	89.84	90.54	91.18	91.06	88.71
LDN	82.56	91.04	91.49	91.33	92.83	93.53	92.71	90.78
LDTP	89.64	92.84	93.74	94.24	94.84	94.81	94.74	93.55
LDSP	85.46	87.81	87.54	86.05	87.21	86.90	85.04	86.57
MGP	91.70	95.21	95.09	95.59	96.48	96.13	95.89	95.16
LDV	83.92	91.84	92.52	91.53	93.55	93.49	93.20	91.44
CPS_ELDP	95.76	95.75	95.83	95.93	95.00	95.78	94.82	95.55
FCCP_LGNP	**97.03**	**97.88**	**98.31**	**99.09**	**98.91**	**98.69**	**98.04**	**98.28**

	N=8							
$(R_l, 8t)$	(1,8)	(2,16)	(3,24)	(4,32)	(5,32)	(6,32)	(7,32)	Avg
LDP	68.55	81.51	90.29	92.53	93.53	94.71	95.69	88.11
ELDP	85.55	92.86	93.39	93.28	93.89	94.80	94.44	92.60
LDN	86.65	94.88	95.03	95.26	96.43	97.08	96.09	94.49
LDTP	92.65	96.71	97.06	96.83	97.59	96.95	97.31	96.44
LDSP	88.76	91.33	91.03	90.49	91.53	91.29	90.00	90.63
MGP	93.79	97.36	97.44	98.08	98.16	98.29	97.64	97.25
LDV	88.10	95.23	96.09	94.53	96.40	96.75	96.36	94.78
CPS_ELDP	97.68	97.60	98.00	97.63	97.68	97.38	96.95	97.56
FCCP_LGNP	**98.13**	**99.64**	**99.44**	**99.63**	**99.81**	**99.68**	**99.20**	**99.36**

(5,32), (6,32) and (7,32), respectively. The Nearest Neighbor Classifier (NNC) was chosen for face recognition. In addition, the noise robustness of the proposed schemes was also evaluated with the related methods. The increasing levels of additive Gaussian white noise model was chosen and the threshold σ was set 0.005, 0.01 and 0.02, respectively. Figure 7 presents some noisy examples. For simplicity, we chose $(R_l, 8t) = (5, 32)$ for noisy-robustness testing.

It is known that the texture descriptors proposed for face recognition can achieve promising results by dividing the face image into non-overlapping regions for feature extraction [7], [35], [47], [51]. Therefore, we further give the comparison of FCCP_LGNP with the state-of-the-art methods in this case, including polynomial contrast binary patterns (PCBP) [7], the mixed neighborhood topology cross decoded patterns (MNTCDP) [47] and the LDP-based methods mentioned above. For simplicity, we chose $(R_l, 8t) = (5, 32)$ for this testing.

In the end, we also test the proposed operator with deep learning methods based on CNN, including VGG16 [52] and ResNet101 [53].

B. RESULTS ON ORL DATABASE
The ORL database is composed of 400 face images taken by 40 different volunteers. Each volunteer contains 10 images, which vary slightly in direction but no significant change in grayscale and expression. Samples of a volunteer are shown in Figure 8.

For the ORL database, to maintain the consistency of data distribution, we adopted stratified sampling to divide the training and test set, that is, we randomly selected $N(N = 4, 6, 8)$ samples from each volunteer for training and the remaining $10-N$ for testing. Each split contains two sub-sets, one for the training and the other for testing. The recognition accuracies averaged by 100 randomly trails were given in Table 1, where 'Avg' denotes the average recognition accuracy. Figure 9 (a) shows the comparison of average recognition accuracies graphically. Figure 9 (b), (c) and (d) denote the comparison of anti-noise performance for $\sigma = 0.005$, $\sigma = 0.01$ and $\sigma = 0.02$, respectively.

From Table 1, the following conclusions can be drawn,
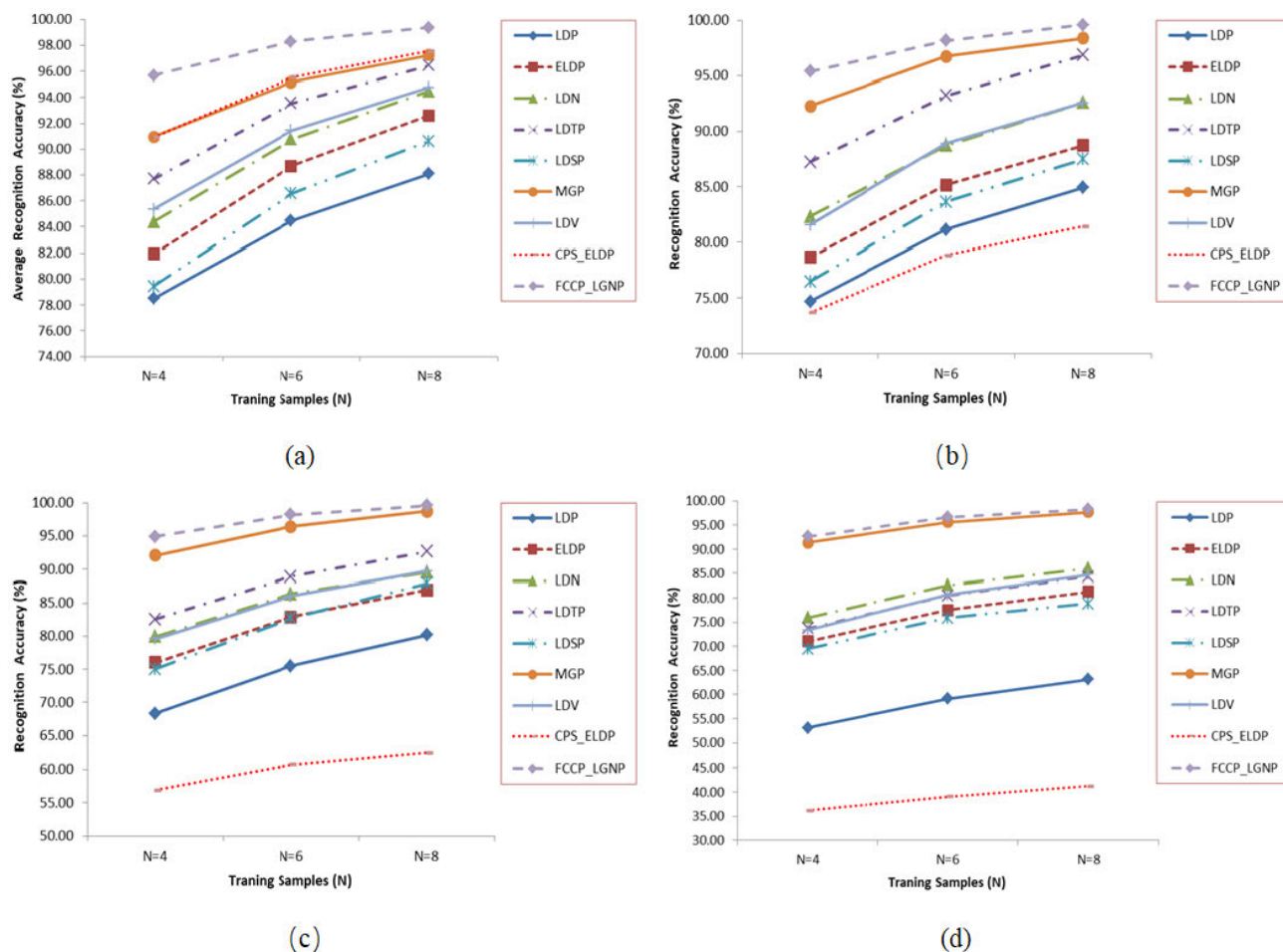- For N = 4, FCCP_LGNP has about 17.17%, 13.77%, 11.31%, 8.00%, 16.24%, 4.71%, 10.33%, and 4.76%

FIGURE 9. The average recognition accuracy and the robustness to noise on ORL database. (a) Average recognition accuracy. (b) $\sigma = 0.005$. (c) $\sigma = 0.01$. (d) $\sigma = 0.02$.

average improvement over LDP, ELDP, LDN, LDTP, LDSP, MGP, LDV, and CPS_ELDP respectively.

- For N = 6, FCCP_LGNP has about 13.82%, 9.57%, 7.5%, 4.73%, 11.70%, 3.12%, 6.84%, and 2.73% average improvement over LDP, ELDP, LDN, LDTP, LDSP, MGP, LDV, and CPS_ELDP respectively.
- For N = 8, FCCP_LGNP has about 11.25%, 6.76%, 4.87%, 2.92%, 8.73%, 2.11%, 4.58%, and 1.80% average improvement over LDP, ELDP, LDN, LDTP, LDSP, MGP, LDV, and CPS_ELDP respectively.

As shown in Figure 9 (a), FCCP_LGNP gives the best scores, followed by CPS_ELDP. It also shows that those methods considering gray variations can achieve relatively better results, such as MGP and LDTP.

From Figure 9 (b), (c), and (d), it can be seen that the noise has different impact on the recognition accuracy of each algorithm. FCCP_LGNP still performs the best, which indicates that the proposed scheme is more robust to noise. The noise has the greatest influence on CPS_ELDP. It means that the CPS strategy is sensitive to noise. Besides CPS_ELDP, LDP is more sensitive to noise than the other operators. Because

MGP combines the local gradient information by the perspective of gray-level changes and MCT transform, it performs better than the other methods except FCCP_LGNP in case of noise.

C. RESULTS ON CALTECH DATABASE
The Caltech database contains 450 faces of 27 individuals under different lighting, expressions and backgrounds. For simplicity, 380 images, which belong to 19 individuals (each has 20 views), were selected for comparison in the experiments. The samples of an individual are shown in Figure 10.

For the CALTECH database, to maintain the consistency of data distribution, we adopted stratified sampling to divide the training and test set, that is, we randomly selected $N(N = 5, 10, 15)$ samples from each volunteer for training and the remaining $20-N$ for testing. Each split contains two sub-sets, one for the training and the other for testing. The recognition accuracies averaged by 100 randomly trails were given in Table 2. Figure 11 (a) shows the comparison of average recognition accuracies. Figure 11 (b), (c) and (d) denote the comparison of anti-noise performance.

FIGURE 10. An individual samples from CALTECH database.

				N=5				
$(R_l, 8t)$	(1,8)	(2,16)	(3,24)	(4,32)	(5,32)	(6,32)	(7,32)	Avg
LDP	33.31	37.09	44.87	52.96	57.05	60.52	62.72	49.79
ELDP	33.81	41.78	48.56	53.43	57.03	61.15	64.35	51.44
LDN	33.86	40.10	47.89	52.07	55.91	58.61	61.90	50.05
LDTP	46.89	55.47	62.26	66.45	70.40	72.83	74.14	64.06
LDSP	45.34	52.59	58.38	63.48	66.05	67.73	69.05	60.37
MGP	48.66	54.51	60.29	63.37	64.72	66.47	67.89	60.84
LDV	36.61	44.51	53.31	58.50	63.34	66.59	69.90	56.11
CPS_ELDP	61.32	59.91	62.29	62.11	63.73	63.52	63.86	62.39
FCCP_LGNP	**53.82**	**63.39**	**71.11**	**75.81**	**77.25**	**78.40**	**79.22**	**71.29**

				N=10				
$(R_l, 8t)$	(1,8)	(2,16)	(3,24)	(4,32)	(5,32)	(6,32)	(7,32)	Avg
LDP	39.81	45.98	53.93	61.68	67.28	71.52	71.23	58.77
ELDP	39.86	50.96	58.84	63.43	67.76	71.15	74.12	60.87
LDN	41.26	47.76	57.06	62.06	66.58	69.41	71.47	59.37
LDTP	56.69	65.21	70.68	75.75	77.57	80.56	81.43	72.56
LDSP	53.32	61.65	67.23	73.01	74.78	77.32	77.91	69.32
MGP	57.85	63.55	69.52	72.72	73.74	75.44	76.13	69.85
LDV	44.70	52.81	63.55	67.71	73.71	76.77	79.50	65.54
CPS_ELDP	71.33	69.85	72.62	72.50	74.03	73.66	74.54	72.65
FCCP_LGNP	**63.45**	**72.18**	**80.26**	**84.93**	**85.64**	**86.25**	**87.17**	**79.98**

				N=15				
$(R_l, 8t)$	(1,8)	(2,16)	(3,24)	(4,32)	(5,32)	(6,32)	(7,32)	Avg
LDP	44.46	51.52	57.78	67.55	72.04	77.20	76.53	63.87
ELDP	43.78	56.33	65.52	70.09	74.81	78.14	80.06	66.96
LDN	46.28	52.31	63.16	68.41	73.18	75.36	77.15	65.12
LDTP	62.08	70.23	75.42	79.44	80.98	84.05	85.69	76.84
LDSP	57.75	67.24	71.42	76.77	78.18	80.95	81.16	73.35
MGP	62.21	68.87	75.05	78.47	78.91	80.03	80.09	74.81
LDV	50.09	58.51	70.02	72.63	79.26	82.15	83.77	70.92
CPS_ELDP	76.54	75.26	79.33	77.52	79.20	79.16	79.25	78.04
FCCP_LGNP	**68.58**	**76.66**	**85.12**	**89.21**	**89.55**	**89.86**	**90.54**	**84.22**

From Table 2, the following conclusions can be drawn,

- For N = 5, FCCP_LGNP has about 21.50%, 19.84%, 21.24%, 7.22%, 10.91%, 10.44%, 15.18%, and 8.89% average improvement over LDP, ELDP, LDN, LDTP, LDSP, MGP, LDV, and CPS_ELDP respectively.
- For N = 10, FCCP_LGNP has about 21.21%, 19.11%, 20.61%, 7.43%, 10.67%, 10.13%, 14.44%, and 7.34% average improvement over LDP, ELDP, LDN, LDTP, LDSP, MGP, LDV, and CPS_ELDP respectively.
- For N = 15, FCCP_LGNP has about 20.35%, 17.26%, 19.10%, 7.37%, 10.86%, 9.41%, 13.30%, and 6.18% average improvement over LDP, ELDP, LDN, LDTP, LDSP, MGP, LDV, and CPS_ELDP respectively.

From Figure 11 (a), it is clear that FCCP_LGNP outperforms the other methods. From Figure 11 (b), (c) and (d), we also observe that FCCP_LGNP has the best ability of robustness to noise.

D. RESULTS ON GERORGIA DATABASE

The GERORGIA database has rich facial expressions and obvious direction changes. It includes 750 color images belonging to 50 individuals, each containing 15 images. Figure 12 shows the samples of an individual.

For the GERORGIA database, to maintain the consistency of data distribution, we adopted stratified sampling to divide the training and test set, that is, we randomly selected $N(N = 5, 9, 13)$ samples from each volunteer for training and the remaining $15-N$ for testing. Each split contains two sub-sets, one for the training and the other for testing. The recognition accuracies averaged by 100 randomly trials were given in Table 3. Figure 13 (a) shows the comparison of average recognition accuracies. Figure 13 (b), (c) and (d) denote the comparison of anti-noise performance.

From Table 3, the following conclusions can be drawn,

- For N = 5, FCCP_LGNP has about 28.54%, 26.96%, 23.39%, 10.01%, 27.20%, 10.17%, 21.65%, and 22.45% average improvement over LDP, ELDP, LDN, LDTP, LDSP, MGP, LDV, and CPS_ELDP respectively.
- For N = 9, FCCP_LGNP has about 26.07%, 24.72%, 21.34%, 8.71%, 26.82%, 8.69%, 19.35%, and 20.58% average improvement over LDP, ELDP, LDN, LDTP, LDSP, MGP, LDV, and CPS_ELDP respectively.
- For N = 13, FCCP_LGNP has about 24.03%, 22.41%, 19.40%, 7.79%, 25.31%, 8.07%, 17.88%, and 19.85% average improvement over LDP, ELDP, LDN, LDTP, LDSP, MGP, LDV, and CPS_ELDP respectively.
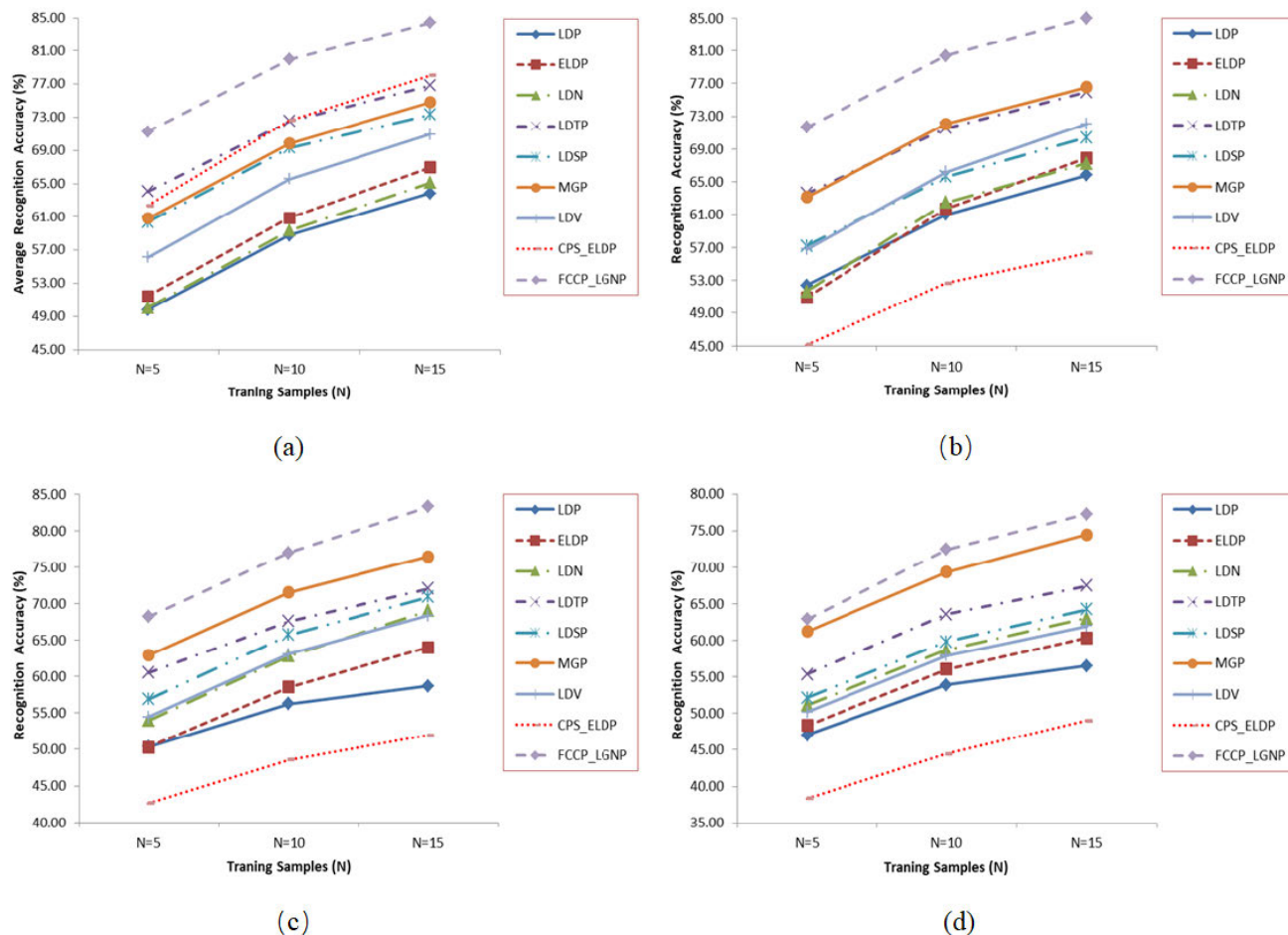
(a)

(b)

(c)

(d)

FIGURE 11. The average recognition accuracy and the robustness to noise on CALTECH database. (a) Average recognition accuracy. (b) $\sigma = 0.005$. (c) $\sigma = 0.01$. (d) $\sigma = 0.02$.

FIGURE 12. An individual samples from GEORGIA database.

As shown in Figure 13 (a), FCCP_LGNP achieves the highest scores. Compared with the results on ORL and CLATECH databases, the performance of CPS_ELDP decreases, which means that the CPS_ELDP is not only

sensitive to noise, but also to expression changes. From Figure 13 (b), (c) and (d), it is worth noting that MGP outperforms FCCP_LGNP for $\sigma = 0.02$. The results indicate that the noise robustness of MGP can be improved by calculating the gray mean repeatedly.

E. RESULTS ON FACE94 DATABASE

The Face94 is a relatively simple database, because it has no obvious changes in direction, expression or background. In the experiment, all male faces from FACE94 were selected as experimental database, which contains 2260 images belonging to 113 individuals. These images depicted slight changes in the face of the subjects when they spoke. Figure 14 shows samples of an individual.

For the FACE94 database, to maintain the consistency of data distribution, we adopted stratified sampling to divide the training and test set, that is, we randomly selected $N(N = 5, 10, 15)$ samples from each volunteer for training and the remaining $20-N$ for testing. Each split contains two sub-sets, one for the training and the other for testing. The recognition accuracies averaged by 100 randomly trials were given in Table 4. Figure 15 (a) visually shows the comparison of
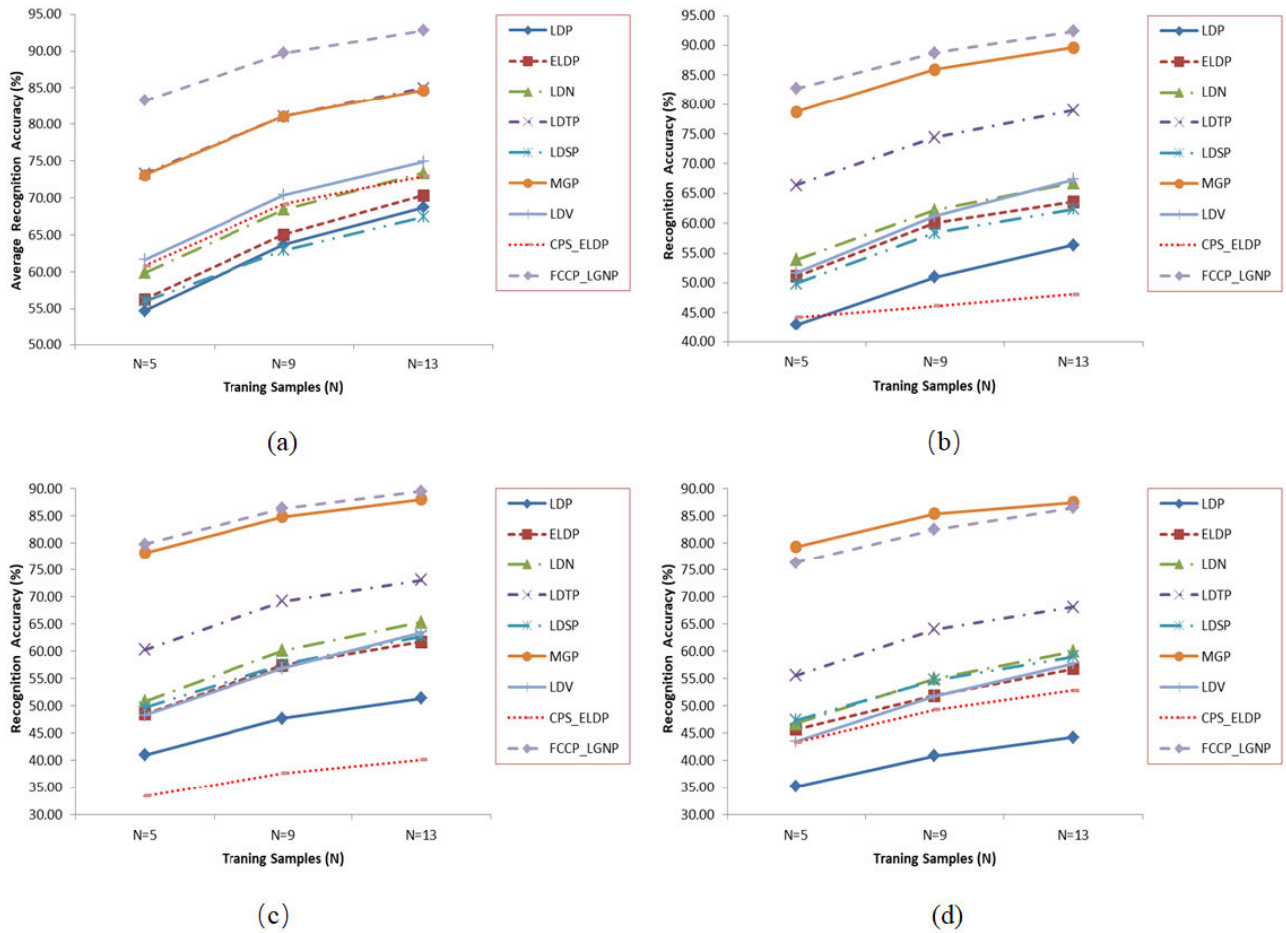
FIGURE 13. The average recognition accuracy and the robustness to noise on GEORGIA database. (a) Average recognition accuracy. (b) $\sigma = 0.005$. (c) $\sigma = 0.01$. (d) $\sigma = 0.02$.

FIGURE 14. An individual samples from FACE94 database.

average recognition accuracies. Figure 15 (b), (c) and (d) denote the comparison of anti-noise performance.

The following conclusions can be drawn from Table 4.

- For N = 5, FCCP_LGNP has about 8.96%, 5.17%, 4.86%, 0.98%, 4.43%, 5.02%, 3.30%, and 4.02%

average improvement over LDP, ELDP, LDN, LDTP, LDSP, MGP, LDV, and CPS_ELDP respectively.

- For N = 10, FCCP_LGNP has about 7.13%, 3.72%, 3.48%, 0.63%, 2.97%, 3.63%, 2.31%, and 2.48% average improvement over LDP, ELDP, LDN, LDTP, LDSP, MGP, LDV, and CPS_ELDP respectively.

- For N = 15, FCCP_LGNP has about 6.34%, 3.03%, 2.81%, 0.48%, 2.34%, 2.99%, 1.79%, and 1.89% average improvement over LDP, ELDP, LDN, LDTP, LDSP, MGP, LDV, and CPS_ELDP respectively.

From Figure 15 (a), we can intuitively observe that the average recognition accuracy of FCCP_LGNP is higher than the other methods. As shown in Figure 15 (b), (c) and (d), FCCP_LGNP still has relatively better anti-noise performance.

F. COMPARING FCCP_LGNP WITH THE STATE-OF-THE-ATR METHODS

It is admitted that the performance of the descriptor depends on the number of non-overlapping regions and the tested databases. In other words, the descriptor may achieve higher score with small number of image blocks on a dataset, whereas it may not obtain good results on the others.

TABLE 3. Experimental results on GEORGIA database.

				N=5				
$(R_l, 8t)$	(1,8)	(2,16)	(3,24)	(4,32)	(5,32)	(6,32)	(7,32)	Avg
LDP	54.41	50.94	52.96	53.86	56.12	56.68	58.07	54.72
ELDP	50.39	54.48	55.87	57.17	57.66	58.62	59.81	56.30
LDN	53.41	57.80	59.45	60.49	61.69	62.88	63.38	59.87
LDTP	65.99	72.86	74.04	74.08	74.86	74.99	75.91	73.25
LDSP	49.94	53.60	54.56	55.54	67.92	55.61	55.22	56.05
MGP	57.17	68.90	72.88	75.76	77.99	79.17	79.72	73.08
LDV	53.66	59.41	60.98	62.45	63.63	65.24	65.92	61.61
CPS_ELDP	59.36	59.48	60.41	61.08	61.55	61.81	61.98	60.81
FCCP_LGNP	**76.58**	**81.50**	**83.70**	**84.38**	**84.96**	**85.58**	**86.11**	**83.26**

				N=9				
$(R_l, 8t)$	(1,8)	(2,16)	(3,24)	(4,32)	(5,32)	(6,32)	(7,32)	Avg
LDP	61.38	58.94	61.49	63.37	66.01	66.89	67.65	63.67
ELDP	58.66	63.35	64.33	65.96	66.20	67.00	69.66	65.02
LDN	61.44	64.78	67.94	68.89	70.55	72.43	72.75	68.40
LDTP	74.07	80.76	82.29	81.69	82.23	82.48	83.68	81.03
LDSP	58.28	61.61	63.63	63.73	64.13	64.63	64.43	62.92
MGP	64.63	77.33	81.45	83.57	85.60	87.03	87.72	81.05
LDV	62.23	67.12	69.22	71.31	72.41	74.92	75.54	70.39
CPS_ELDP	68.11	67.17	68.45	68.97	70.39	70.43	70.59	69.16
FCCP_LGNP	**84.12**	**88.59**	**89.59**	**90.85**	**91.03**	**92.00**	**92.01**	**89.74**

				N=13				
$(R_l, 8t)$	(1,8)	(2,16)	(3,24)	(4,32)	(5,32)	(6,32)	(7,32)	Avg
LDP	65.84	63.08	66.00	68.04	71.68	73.06	73.44	68.73
ELDP	64.52	68.34	69.48	71.25	71.25	72.13	75.46	70.35
LDN	66.68	69.13	72.63	74.24	75.36	77.61	77.88	73.36
LDTP	79.02	84.52	85.86	85.84	86.34	86.34	86.92	84.98
LDSP	63.08	65.40	68.30	69.62	68.36	67.84	69.58	67.45
MGP	68.66	81.42	85.70	87.42	89.30	89.80	90.56	84.69
LDV	66.68	71.54	73.41	75.79	76.49	79.79	80.44	74.88
CPS_ELDP	71.24	72.40	73.22	71.70	73.50	74.06	74.26	72.91
FCCP_LGNP	**87.74**	**91.72**	**93.16**	**93.82**	**94.42**	**94.56**	**93.92**	**92.76**

TABLE 4. Experimental results on FACE94 database.

				N=5				
$(R_l, 8t)$	(1,8)	(2,16)	(3,24)	(4,32)	(5,32)	(6,32)	(7,32)	Avg
LDP	59.04	82.85	90.03	91.43	91.89	92.13	92.01	85.63
ELDP	77.66	88.69	90.91	91.87	92.20	92.34	92.25	89.42
LDN	76.18	89.40	92.06	92.51	92.63	92.76	92.61	89.73
LDTP	89.88	93.77	94.21	94.45	94.51	94.31	94.15	93.61
LDSP	85.90	90.25	90.79	91.18	91.22	90.85	90.92	90.16
MGP	72.80	88.79	91.06	92.90	93.46	94.06	93.92	89.57
LDV	80.77	91.37	92.94	93.27	93.59	93.63	93.46	91.29
CPS_ELDP	89.20	89.29	90.82	90.91	91.09	91.35	91.31	90.57
FCCP_LGNP	**93.73**	**94.53**	**94.61**	**95.00**	**94.84**	**94.73**	**94.68**	**94.59**

				N=10				
$(R_l, 8t)$	(1,8)	(2,16)	(3,24)	(4,32)	(5,32)	(6,32)	(7,32)	Avg
LDP	65.62	87.95	94.15	95.73	95.94	96.24	95.96	90.23
ELDP	82.78	93.25	94.97	95.84	96.17	96.36	96.15	93.64
LDN	82.42	93.65	95.86	96.14	96.39	96.45	96.28	93.88
LDTP	93.98	96.99	97.11	97.35	97.21	97.26	97.22	96.73
LDSP	90.80	94.66	94.84	95.09	95.27	95.05	94.99	94.39
MGP	79.28	93.73	95.36	96.28	96.85	97.20	97.44	93.73
LDV	86.47	95.31	96.42	96.69	96.88	96.85	96.75	95.05
CPS_ELDP	93.79	93.81	95.03	95.03	95.51	95.49	95.52	94.88
FCCP_LGNP	**96.75**	**97.40**	**97.38**	**97.49**	**97.55**	**97.46**	**97.48**	**97.36**

				N=15				
$(R_l, 8t)$	(1,8)	(2,16)	(3,24)	(4,32)	(5,32)	(6,32)	(7,32)	Avg
LDP	69.20	90.11	95.60	96.97	97.23	97.39	97.11	91.94
ELDP	85.01	94.98	96.53	97.29	97.51	97.84	97.56	95.25
LDN	85.10	95.45	97.12	97.39	97.75	97.84	97.62	95.47
LDTP	95.39	98.12	98.14	98.25	98.22	98.25	98.23	97.80
LDSP	92.84	96.24	96.11	96.43	96.71	96.61	96.66	95.94
MGP	82.25	95.64	97.44	97.43	97.76	98.15	98.36	95.29
LDV	88.95	96.78	97.67	97.93	98.01	98.08	98.02	96.49
CPS_ELDP	95.55	95.41	96.35	96.52	96.87	97.09	96.95	96.39
FCCP_LGNP	**97.98**	**98.25**	**98.33**	**98.34**	**98.41**	**98.30**	**98.36**	**98.28**

In addition, more blocks don't always bring good results. Maybe, it only leads to the increasing of the computational complexity.

On ORL database, the number of blocks is set 9 as that of the MNTCDP [47]. In addition, for the balance of the performance and the computational complexity, a series of extensive experiments were carried out on CALTECH, GRORGIA and FACE94 databases, and the results show that the evaluated operators perform better when the images are divided into 12, 6, and 9 blocks, respectively. The recognition accuracies averaged by 10 randomly trials were given in Table 5, where the results of MNTCDP are taken directly from the cited paper [47]. Figure 16 reports the results visually.

From Table 5, it can be clearly seen that FCCP_LGNP achieves the highest accuracies on the more complex CALTECH and GEORGIA databases, which denotes that the proposed method is more robust and powerful for the databases with different lighting, expressions and backgrounds. MNTCDP performs a little better than FCCP_LGNP on ORL database. However, the feature dimensionality of MNTCDP is as high as 9216 (1024×9), while that of FCCP_LGNP is only 1008 (112 × 9). In the experiments, we also found that the recognition rates of FCCP_LGNP could reach 99.21%, 100% and 100% ($N = 4, 6, 8$) when the number blocks is 2.
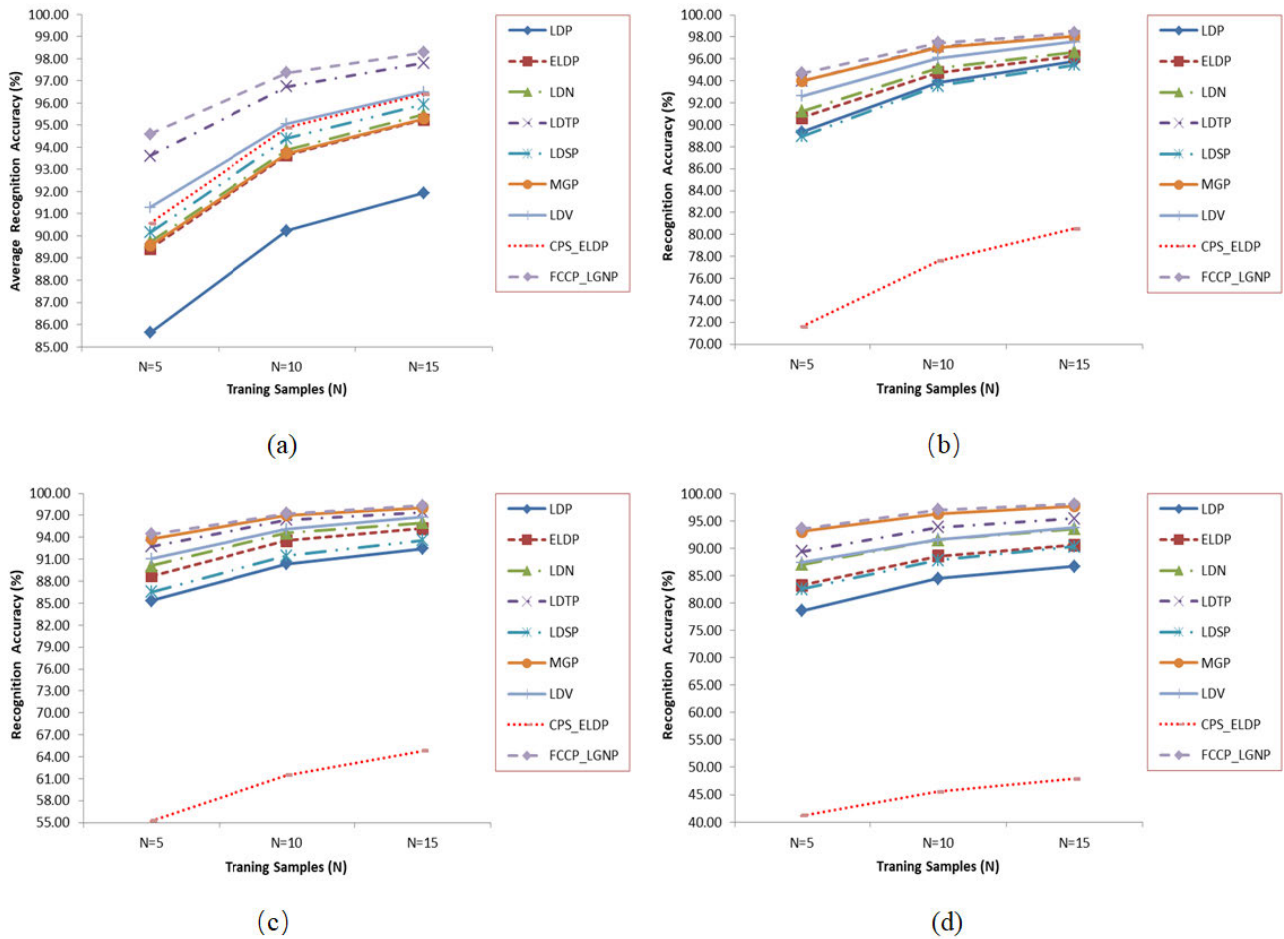
FIGURE 15. The average recognition accuracy and the robustness to noise on FACE94 database. (a) Average recognition accuracy. (b) $\sigma = 0.005$. (c) $\sigma = 0.01$. (d) $\sigma = 0.02$.

TABLE 5. Comparison of FCCP_LGNP and the state-of-the-art methods.

Operators	ORL			CALTECH			GEORGIA			FACE94		
	N=4	N=6	N=8	N=5	N=10	N=15	N=5	N=9	N=13	N=5	N=10	N=15
FCCP_LGNP	98.46	99.69	**100.00**	**95.44**	**98.37**	**99.68**	**90.20**	**95.67**	**98.20**	97.81	**99.16**	**99.47**
MGP	97.17	98.81	99.63	90.70	95.63	97.68	81.64	89.17	92.50	**98.22**	99.11	99.43
MNTCDP	**99.67**	**100.00**	100.00	—	—	—	—	—	—	—	—	—
LDTP	96.38	98.38	99.50	93.16	97.58	98.32	84.82	90.97	94.30	97.20	98.73	99.36
CPS_ELDP	97.04	98.81	99.75	83.72	93.37	96.63	83.54	90.43	93.10	94.55	97.83	98.02
LDSP	93.75	97.06	98.75	93.65	97.74	98.95	76.48	84.87	91.10	95.20	97.87	98.73
LDN	95.83	97.88	98.50	92.56	96.68	98.00	79.62	87.13	91.50	96.27	98.12	98.85
ELDP	95.63	98.44	98.88	92.18	96.58	98.11	79.46	87.00	91.10	95.68	97.91	98.85
LDP	94.75	97.81	98.50	87.86	93.53	97.26	76.24	85.97	89.60	96.13	98.41	98.89
LDV	96.33	99.00	**100.00**	93.05	97.63	98.77	80.50	88.07	92.00	96.42	98.48	98.99
PCBP	97.63	99.38	**100.00**	84.78	93.37	96.42	80.04	87.53	91.50	95.10	97.68	98.60

G. COMPARING FCCP_LGNP WITH DEEP LEARNING METHODS

In recent years, the deep learning methods based on CNN have been studied widely and applied in various fields,

including face recognition. In this part, two classic networks, VGG16 and ResNet101, were chosen for comparison. Because of the numbers of the four face databases are too limited to evaluate the performance of VGG16 and
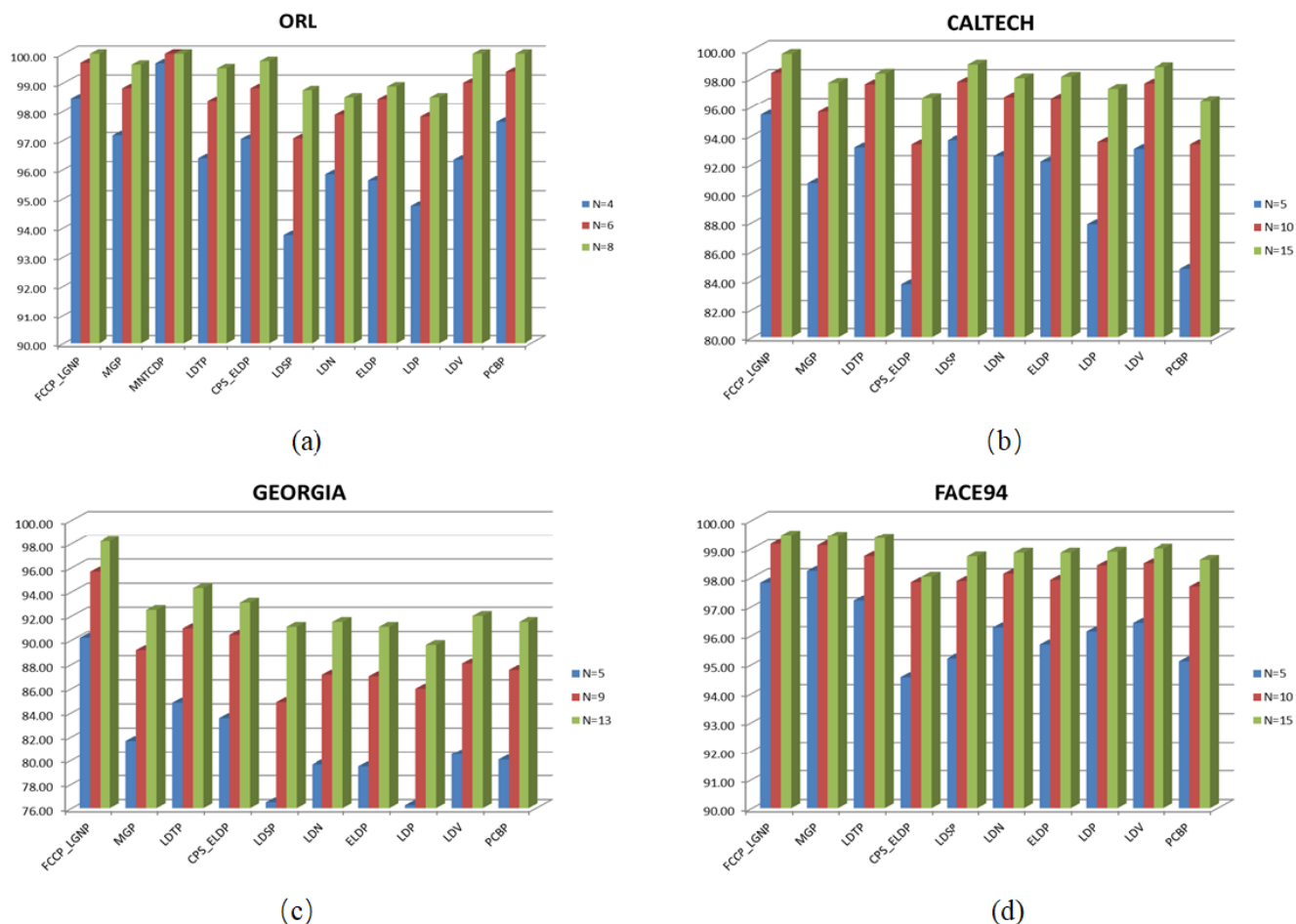
FIGURE 16. The average recognition accuracy on ORL, CALTECH, GEORGIA and FACE94 databases. (a) ORL. (b) CALTECH. (c) GEORGIA. (d) FACE94.

TABLE 6. Comparison with VGG16 and ResNet101.

Operators	ORL			CALTECH			GEORGIA			FACE94		
	N=4	N=6	N=8	N=5	N=10	N=15	N=5	N=9	N=13	N=5	N=10	N=15
VGG16	94.20	99.40	**100.00**	64.00	90.10	98.20	75.00	91.50	98.30	95.50	**100.00**	**100.00**
ResNet101	96.00	**100.00**	**100.00**	75.60	95.60	**99.80**	84.10	95.30	**99.60**	97.70	**100.00**	**100.00**
FCCP_LGNP	**98.46**	99.69	**100.00**	**95.44**	**98.37**	99.68	**90.20**	**95.67**	98.20	**97.81**	99.16	99.47

ResNet101, we used random flip and random shift to realize data augmentation [45]. To avoid over-fitting, the order of training sets and test sets were disturbed.

For VGG16, the rectified linear unit (ReLU) and dropout strategy were adopted to improve its classification effect. The global pool was used in ResNet101 to enhance the generalization ability and robustness. Besides, we applied batch normalization (BN) both in VGG16 and ResNet101 to accelerate convergence. In the experiment, stochastic gradient descent (SGD) with momentum was chosen as optimizer. The results were shown in Table 6. For FCCP_LGNP, we directly use the experimental results given in Table 5.

Clearly, the performance of FCCP_LGNP is better than the deep-learning methods, VGG16 and ResNet101, with small training data. With the increase of training data, VGG16 and ResNet101 show a little better than the proposed FCCP_LGNP. However, they need high computing cost and long running time to learn the optimal model. In addition, they achieve such results by the data augmentation.

V. CONCLUSION

A new descriptor, named FCCP_LGNP, is proposed in this paper for face recognition based on the LDP-based methods. Unlike the traditional approaches, the proposed scheme

encodes the gradient values instead of the edge responses to achieve robustness to noise and gray-level changes. In addition, the Kirsch template is replaced by the Sobel operators to reduce the computational complexity. Further, the FCCP strategy is introduced to enhance the ability of CCP. Experiments on multiple face databases show that the proposed scheme gives better scores than the state-of-the-art methods mentioned in the paper. In further research, we will consider how to combine FCCP_LGNP with deep learning technology to further improve its accuracy, and expand its scope of application.

REFERENCES

[1] M. Singh, R. Singh, and A. Ross, "A comprehensive overview of biometric fusion," *Inf. Fusion*, vol. 52, pp. 187–205, Dec. 2019.

[2] N. Zhou, A. G. Constantinides, G. Huang, and S. Zhang, "Face recognition based on an improved center symmetric local binary pattern," *Neural Comput. Appl.*, vol. 30, no. 12, pp. 3791–3797, Apr. 2017, doi: 10.1007/s00521-017-2963-2.

[3] S. Y. Wong, K. S. Yap, Q. Zhai, and X. Li, "Realization of a hybrid locally connected extreme learning machine with DeepID for face verification," *IEEE Access*, vol. 7, pp. 70447–70460, 2019.

[4] S. Z. Li, A. K. Jain, Y. L. Tian, T. Kanade, and J. F. Cohn, "Facial expression analysis," in *Handbook of Face Recognition*. New York, NY, USA: Springer-Verlag, 2005, pp. 247–275.

[5] I. Kotsia and I. Pitas, "Facial expression recognition in image sequences using geometric deformation features and support vector machines," *IEEE Trans. Image Process.*, vol. 16, no. 1, pp. 172–187, Jan. 2007.

[6] C. Shan, S. Gong, and P. W. McOwan, "Facial expression recognition based on local binary patterns: A comprehensive study," *Image Vis. Comput.*, vol. 27, no. 6, pp. 803–816, May 2009.

[7] Z. Xu, Y. Jiang, Y. Wang, Y. Zhou, W. Li, and Q. Liao, "Local polynomial contrast binary patterns for face recognition," *Neurocomputing*, vol. 355, pp. 1–12, Aug. 2019.

[8] M.-D. Yuan, D.-Z. Feng, Y. Shi, and W.-J. Liu, "Dimensionality reduction by collaborative preserving Fisher discriminant analysis," *Neurocomputing*, vol. 356, pp. 228–243, Sep. 2019.

[9] Y.-F. Yu, D.-Q. Dai, C.-X. Ren, and K.-K. Huang, "Discriminative multi-scale sparse coding for single-sample face recognition with occlusion," *Pattern Recognit.*, vol. 66, pp. 302–312, Jun. 2017.

[10] M. Zhao, Z. Jia, and D. Gong, "Improved two-dimensional quaternion principal component analysis," *IEEE Access*, vol. 7, pp. 79409–79417, 2019.

[11] Z. Lei, X. Zhang, S. Yang, Z. Ren, and O. F. Akindipe, "RFR-DLVT: A hybrid method for real-time face recognition using deep learning and visual tracking," *Enterprise Inf. Syst.*, to be published, doi: 10.1080/17517575.2019.1668964.

[12] T. Ojala, M. Pietikäinen, and D. Harwood, "A comparative study of texture measures with classification based on featured distributions," *Pattern Recognit.*, vol. 29, no. 1, pp. 51–59, Jan. 1996.

[13] L. Nanni, A. Lumini, and S. Brahnam, "Survey on LBP based texture descriptors for image classification," *Expert Syst. Appl.*, vol. 39, no. 3, pp. 3634–3641, Feb. 2012.

[14] Z. Pan, Z. Li, H. Fan, and X. Wu, "Feature based local binary pattern for rotation invariant texture classification," *Expert Syst. Appl.*, vol. 88, pp. 238–248, Dec. 2017.

[15] M. Hu, Y. Zheng, C. Yang, X. Wang, L. He, and F. Ren, "Facial expression recognition using fusion features based on center-symmetric local octonary pattern," *IEEE Access*, vol. 7, pp. 29882–29890, 2019.

[16] T. Song, L. Xin, C. Gao, G. Zhang, and T. Zhang, "Grayscale-inversion and rotation invariant texture description using sorted local gradient pattern," *IEEE Signal Process. Lett.*, vol. 25, no. 5, pp. 625–629, May 2018.

[17] T. Ojala, M. Pietikainen, and T. Maenpaa, "Multiresolution gray-scale and rotation invariant texture classification with local binary patterns," *IEEE Trans. Pattern Anal. Mach. Intell.*, vol. 24, no. 7, pp. 971–987, Jul. 2002.

[18] X. Tan and B. Triggs, "Enhanced local texture feature sets for face recognition under difficult lighting conditions," *IEEE Trans. Image Process.*, vol. 19, no. 6, pp. 1635–1650, Jun. 2010.

[19] I. Choi and D. Kim, "A variety of local structure patterns and their hybridization for accurate eye detection," *Pattern Recognit.*, vol. 61, pp. 417–432, Jan. 2017.

[20] M. Subrahmanyam, R. P. Maheshwari, and R. Balasubramanian, "Local maximum edge binary patterns: A new descriptor for image retrieval and object tracking," *Signal Process.*, vol. 92, no. 6, pp. 1467–1479, Jun. 2012.

[21] J. Sun, G. Fan, and X. Wu, "New local edge binary patterns for image retrieval," in *Proc. IEEE Int. Conf. Image Process.*, Sep. 2013, pp. 1467–1479.

[22] S. Murala, R. P. Maheshwari, and R. Balasubramanian, "Local tetra patterns: A new feature descriptor for content-based image retrieval," *IEEE Trans. Image Process.*, vol. 21, no. 5, pp. 2874–2886, May 2012.

[23] T. Jabid, M. H. Kabir, and O. Chae, "Local directional pattern (LDP) for face recognition," in *Dig. Tech. Papers Int. Conf. Consum. Electron. (ICCE)*, Jan. 2010, pp. 329–330.

[24] F. Zhong and J. Zhang, "Face recognition with enhanced local directional patterns," *Neurocomputing*, vol. 119, pp. 375–384, Nov. 2013.

[25] A. R. Rivera, J. R. Castillo, and O. O. Chae, "Local directional number pattern for face analysis: Face and expression recognition," *IEEE Trans. Image Process.*, vol. 22, no. 5, pp. 1740–1752, May 2013.

[26] A. Ramírez Rivera, J. Rojas Castillo, and O. Chae, "Local directional texture pattern image descriptor," *Pattern Recognit. Lett.*, vol. 51, pp. 94–100, Jan. 2015.

[27] A. Ramirez Rivera, J. A. Rojas Castillo, and O. Chae, "Recognition of face expressions using local principal texture pattern," in *Proc. 19th IEEE Int. Conf. Image Process.*, Sep. 2012, pp. 2609–2612.

[28] J. Li, N. Sang, and C. Gao, "LEDTD: Local edge direction and texture descriptor for face recognition," *Signal Process., Image Commun.*, vol. 41, pp. 40–45, Feb. 2016.

[29] X. Krizhevsky, I. Sutskever, and G. E. Hinton, "Imagenet classification with deep convolutional neural networks," in *Proc. Adv. Neural Inf. Process. Syst.*, 2012, pp. 1097–1105.

[30] M. O. Oloyede, G. P. Hancke, and H. C. Myburgh, "Improving face recognition systems using a new image enhancement technique, hybrid features and the convolutional neural network," *IEEE Access*, vol. 6, pp. 75181–75191, 2018.

[31] N. Kanopoulos, N. Vasanthavada, and R. L. Baker, "Design of an image edge detection filter using the sobel operator," *IEEE J. Solid-State Circuits*, vol. 23, no. 2, pp. 358–367, Apr. 1988.

[32] F. Makhmudkhujaev, M. T. B. Iqbal, B. Ryu, and O. Chae, "Local directional-structural pattern for person-independent facial expression recognition," *TURKISH J. Electr. Eng. Comput. Sci.*, vol. 27, no. 1, pp. 516–531, Jan. 2019.

[33] X. Wu and J. Sun, "Face recognition based on multi-scale local directional value," *Multimedia Tools Appl.*, to be published, doi: 10.1007/s11042-019-08245-1.

[34] X. Wu and J. Sun, "Joint-scale LBP: A new feature descriptor for texture classification," *Vis. Comput.*, vol. 33, no. 3, pp. 317–329, Dec. 2015.

[35] J. Sun, G. Fan, L. Yu, and X. Wu, "Concave-convex local binary features for automatic target recognition in infrared imagery," *EURASIP J. Image Video Process.*, vol. 2014, no. 1, pp. 1–13, Apr. 2014.

[36] L. A. Zadeh, "Fuzzy sets as a basis for a theory of possibility," *Fuzzy Sets Syst.*, vol. 100, pp. 9–34, Jan. 1999.

[37] D. K. Iakovidis, E. Keramidas, and D. Maroulis, "Fuzzy local binary patterns for ultrasound texture characterizations," in *Proc. 5th Int. Conf. Image Anal. Recognit.* Povoa de Varzim, Portugal: Springer, 2008, pp. 750–759.

[38] T. Ahonen, A. Hadid, and M. Pietikinen, "Face recognition with local binary patterns," in *Proc. ECCV*, 2004, pp. 469–481.

[39] Z. Pan, X. Wu, and Z. Li, "Central pixel selection strategy based on local gray-value distribution by using gradient information to enhance LBP for texture classification," *Expert Syst. Appl.*, vol. 120, pp. 319–334, Apr. 2019.

[40] F. S. Samaria and A. C. Harter, "Parameterisation of a stochastic model for human face identification," in *Proc. IEEE Workshop Appl. Comput. Vis.*, Dec. 1994, pp. 138–142.

[41] R. Fergus, P. Perona, and A. Zisserman, "Object class recognition by unsupervised scale-invariant learning," in *Proc. IEEE Conf. Comput. Vis. Pattern Recognit.*, vol. 2, Jun. 2003, pp. 264–271.

[42] (2007). *Georgia Tech Face Database*. [Online]. Available: http://www.anefian.com/face_reco.htm

[43] (Mar. 2003). *Yale Face Database*. [Online]. Available: http://cvc.cs.yale.edu/cvc/projects/yalefaces/yalefaces.html

[44] (2007). *Computer Vision Science Research Projects*. [Online]. Available: http://cswww.essex.ac.uk/mv/allfaces/index.html

[45] Y.-D. Zhang, C. Pan, J. Sun, and C. Tang, "Multiple sclerosis identification by convolutional neural network with dropout and parametric ReLU," *J. Comput. Sci.*, vol. 28, pp. 1–10, Sep. 2018.

[46] Y. El Merabet, Y. Ruichek, and A. El Idrissi, "Attractive-and-repulsive center-symmetric local binary patterns for texture classification," *Eng. Appl. Artif. Intell.*, vol. 78, pp. 158–172, Feb. 2019.

[47] M. Kas, Y. El Merabet, Y. Ruichek, and R. Messoussi, "Mixed neighborhood topology cross decoded patterns for image-based face recognition," *Expert Syst. Appl.*, vol. 114, pp. 119–142, Dec. 2018.

[48] M. Kas, Y. El-merabet, Y. Ruichek, and R. Messoussi, "A comprehensive comparative study of handcrafted methods for face recognition LBP-like and non LBP operators," *Multimedia Tools Appl.*, vol. 79, nos. 1–2, pp. 375–413, Aug. 2019.

[49] K. Slimani, M. Kas, Y. El Merabet, R. Messoussi, and Y. Ruichek, "Facial emotion recognition: A comparative analysis using 22 LBP variants," in *Proc. 2nd Medit. Conf. Pattern Recognit. Artif. Intell. (MedPRAI)*, Mar. 2018, pp. 88–94.

[50] R. C. Gonzalez and R. E. Woods, "Gray transformation and spatial filtering," in *Digital Image Processing*, 3rd ed. Upper Saddle River, NJ, USA: Prentice-Hall, 2006, pp. 187–189.

[51] B. Yang and S. Chen, "A comparative study on local binary pattern (LBP) based face recognition: LBP histogram versus LBP image," *Neurocomputing*, vol. 120, pp. 365–379, Nov. 2013.

[52] K. Simonyan and A. Zisserman, "Very deep convolutional networks for large-scale image recognition," in *Proc. Int. Conf. Learn. Represent.*, 2015, pp. 1–14.

[53] K. He, X. Zhang, S. Ren, and J. Sun, "Deep residual learning for image recognition," in *Proc. IEEE Conf. Comput. Vis. Pattern Recognit. (CVPR)*, Jun. 2016, pp. 770–778.

YANAN LV is currently pursuing the master's degree in computer technology with Henan Polytechnic University. His major research interests are image processing and pattern recognition.

CHAOSHENG TANG received the Ph.D. degree from Yanshan University. He is currently a Lecturer with Henan Polytechnic University. His major research interests are deep learning, large scale data mining, and complex networks.

HAIFENG SIMA received the Ph.D. degree from the Beijing Institute of Technology. He is currently a Lecturer with Henan Polytechnic University. His major research interests are image processing and pattern recognition.

JUNDING SUN received the Ph.D. degree in computer application from Xidian University, in 2005. He is currently a Professor with Henan Polytechnic University. His major research interests are image processing, image retrieval, pattern recognition, and multimedia application.

XIAOSHENG WU received the B.S. and M.S. degrees in computer application from Henan Polytechnic University, in 1998 and 2010, respectively. She is currently an Associate Professor with Henan Polytechnic University. Her research interests include image retrieval and pattern recognition.

● ● ●